Inorg. Chem. **2002**, *41*, 1464–1473

Thermodynamics, Kinetics, and Mechanism of the Stepwise Dissociation and Formation of Tris(L-lysinehydroxamato)iron(III) in Aqueous Acid

Joseph I. Wirgau, Ivan Spasojević, Hakim Boukhalfa, Ines Batinić-Haberle, and Alvin L. Crumbliss*

Department of Chemistry, Duke University, Box 90346, Durham, North Carolina 27708-0346

Received September 18, 2001

pK_a values for the hydroxamic acid, α-NH_3^+, and ϵ-NH_3^+ groups of L-lysinehydroxamic acid (LyHA, H_3L^{2+}) were found to be 6.87, 8.89, and 10.76, respectively, in aqueous solution ($I = 0.1$ M, $NaClO_4$) at 25 °C. O,O coordination to Fe(III) by LyHA is supported by H^+ stoichiometry, UV–vis spectral shifts, and a shift in ν_{CO} from 1648 to 1592 cm^{-1} upon formation of mono(L-lysinehydroxamato)tetra(aquo)iron(III) ($Fe(H_2L)(H_2O)_4^{4+}$). The stepwise formation of tris(L-lysinehydroxamato)iron(III) from $Fe(H_2O)_6^{3+}$ and H_3L^{2+} was characterized by spectrophotometric titration, and the values for log β_1, log β_2, and log β_3 are 6.80(9), 12.4(2), and 16.1(2), respectively, at 25 °C and $I = 2.0$ M ($NaClO_4$). Stopped-flow spectrophotometry was used to study the proton-driven stepwise ligand dissociation kinetics of tris(L-lysinehydroxamato)iron(III) at 25 °C and $I = 2.0$ M ($HClO_4/NaClO_4$). Defining k_n and k_{-n} as the stepwise ligand dissociation and association rate constants and n as the number of bound LyHA ligands, k_3, k_{-3}, k_2, k_{-2}, k_1, and k_{-1} are 3.0×10^4, 2.4×10^1, 3.9×10^2, 1.9×10^1, 1.4×10^{-1}, and 1.2×10^{-1} M^{-1} s^{-1}, respectively. These rate and equilibrium constants are compared with corresponding constants for Fe(III) complexes of acetohydroxamic acid (AHA) and *N*-methylacetohydroxamic acid (NMAHA) in the form of a linear free energy relationship. The role of electrostatics in these complexation reactions to form the highly charged $Fe(LyHA)_3^{6+}$ species is discussed, and an interchange mechanism mediated by charge repulsion is presented. The reduction potential for tris(L-lysinehydroxamato)iron(III) is −214 mV (vs NHE), and a comparison to other hydroxamic acid complexes of Fe(III) is made through a correlation between $E_{1/2}$ and pFe.

Introduction

Iron is the second most abundant metal on the earth's surface and is essential for almost all living cells. Microorganisms are forced to synthesize low-molecular-weight chelating agents to selectively bind and transport iron due to the low solubility of Fe(III) hydroxy species at physiological pH ($K_{sp} \approx 10^{-39}$). These chelating agents, siderophores, bind iron by utilizing one or more of three bidentate moieties, α-hydroxycarboxylic acids, catechols, or hydroxamic acids.[1]

Synthetic hydroxamic acids have been used to model siderophores[2−6] and have received much clinical attention for the treatment of iron-overload disorders,[6−10] lung silicosis,[11,12] and use as antimalarials[13,14] and antibacterials.[6,15] The hydroxamic acid derivatives of amino acids were first studied for their ability to inhibit metalloproteases.[16] Since then, they

* To whom correspondence should be addressed. E-mail: alc@chem.duke.edu. Fax: (919) 660-1605.

(1) Albrecht-Gary, A.-M.; Crumbliss, A. L. *Met. Ions Biol. Syst.* **1998**, *35*, 239.
(2) Raymond, K. N.; Muller, G.; Matzanke, B. F. *Top. Curr. Chem.* **1984**, *123*, 49.
(3) Crumbliss, A. L. In *CRC Handbook of Microbial Iron Chelates*; Winkelmann, G., Ed.; CRC Press: New York, 1991; p 177.
(4) van der Helm, D.; Jalal, M. A. F.; Hossain, M. B. In *Iron Transport in Microbes, Plants, and Animals*; Winkelmann, G., van der Helm, D., Neilands, J. B., Eds.; VCH: New York, 1987; Chapter 9.
(5) Crumbliss, A. L. *Coord. Chem. Rev.* **1990**, *105*, 155.
(6) Matzanke, B. F.; Mueller-Matzanke, G.; Raymond, K. N. In *Iron Carriers and Iron Proteins*; Loeher, T. M., Ed.; VCH: New York, 1989; Chapter 1.
(7) Anderson, W. F. In *Inorganic Chemistry in Biology and Medicine*; Martell, A. E., Ed.; American Chemical Society: Washington, DC, 1980; Vol. 140, p 251.
(8) Martell, A. E., Anderson, W. F., Badman, D. G., Eds. *Development of Iron Chelators for Clinical Use*; Elsevier: New York, 1981.
(9) Pitt, C. G.; Martell, A. E. *ACS Symp. Ser.* **1980**, *140*, 279.
(10) Bergeron, R. J., Brittenham, G. M., Eds. *The Development of Iron Chelators for Clinical Use*; CRC Press: London, 1994.
(11) Ghio, A. J.; Kennedy, T. P.; Whorton, A. R.; Crumbliss, A. L.; Hatch, G. E.; Hoidal, J. R. *Am. J. Physiol.* **1992**, *263*, L511.
(12) Ghio, A. J.; Sonehuerner, J.; Steel, M. P.; Crumbliss, A. L. *Arch. Biochem. Biophys.* **1994**, *315*, 219.
(13) Hynes, J. B.; Hack, L. G. *J. Med. Chem.* **1972**, *15*, 1194.
(14) Gordeuk, V. R.; Brittenham, G. M.; Thuma, P. E. In *The Development of Iron Chelators for Clinical Use*; Bergeron, R. J., Brittenham, G. M., Eds.; CRC Press: London, 1994; p 111.

10.1021/ic0109795 CCC: $22.00
Published on Web 02/19/2002

have been studied in regard to hepatic coma treatment,[17] urolithiasis therapuetics,[18] and the selective removal of heavy metal ions from aqueous solution.[19]

Herein is reported the Fe(III) coordination chemistry of the aminohydroxamic acid L-lysinehydroxamic acid (LyHA, H_3L^{2+}, **I**), including the thermodynamics, kinetics, and mechanism of the stepwise chelation/dechelation process. The protonation constants of LyHA are also reported. The data are analyzed to deduce which of the eight possible Fe(III)-binding modes for LyHA (with the four most probable illustrated as structures **IIa** through **IId** where R = $(CH_2)_4NH_3^+$) occur in solution.

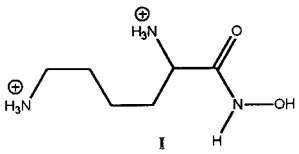

I

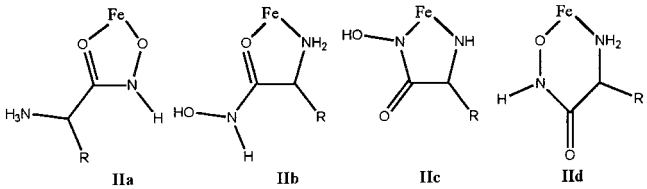

IIa IIb IIc IId

Experimental Section

Materials. The purity of LyHA (Sigma) was checked potentiometrically.[20] NaOH (Fischer reagent with 0.03% carbonate) diluted under an inert atmosphere and standardized with oven-dried potassium hydrogen phthalate, was used for pH measurements. $Fe(ClO_4)_3$ (Aldrich) was used to prepare a stock solution of $Fe(ClO_4)_3$ in 0.1 M $HClO_4$ as previously described.[21] $NaClO_4$ (Aldrich (99%)) was dissolved in doubly deionized water to prepare a 2.0 M stock solution, which was filtered to remove insoluble impurities. $HClO_4$ solutions used in the stopped-flow experiments were dilutions of a 1.92 M $HClO_4$ stock solution that was prepared as previously described.[22] ICN Biomedicals D_2O (98%), sodium (99%), and anhydrous $FeCl_3$ (Aldrich (98%)) were used in sample preparation for IR spectrophotometric measurements.

Methods. pH measurements were carried out using a Corning 250 pH/ion meter equipped with an Orion ROSS pH electrode filled with 3.0 M NaCl solution and standardized by two buffers. The internal calibration of the electrode was performed by SUPERQUAD-MAGEC[23] cycling refinement[24] using data obtained in separate experiments in which $HClO_4$ and LyHA were titrated with NaOH.

Ligand protonation constants were determined by titrations performed in the pH range from 6.23 to 11.36 with 0.01 M NaOH in the absence of Fe(III). The LyHA concentrations used varied from 1.05×10^{-2} to 4.14×10^{-2} M, and the ionic strength was kept constant at 0.1 M by $NaClO_4$. All measurements were made under a purified N_2 atmosphere. The measuring system was thermostated at 25.0(1) °C. SUPERQUAD calculations of these titrations using an electrode calibration obtained by MAGEC yielded refined pK_a values.[23]

The number of protons released upon Fe(III) chelation was determined by a Hill plot under the conditions of 0.0128 M $Fe(ClO_4)_3$, 0.5 mM LyHA, and 0.026−0.313 M $HClO_4$. The first stability constant was determined through the Benesi−Hildebrand method[25] ($[Fe^{3+}]_{tot}$ ranged from 5.01×10^{-3} to 0.076 M in 0.096 M $HClO_4$ and 5×10^{-4} M LyHA). The stability constants for the bis- and tris(L-lysinehydroxamato)iron(III) complexes were obtained from the spectrophotometric titration of a solution containing LyHA and Fe(III) in the pH region of 1.19−8.16 ($[Fe^{3+}]_{tot}$ = 0.1 mM and $[H_3L^{2+}]_{tot}$ = 0.96 mM). Electronic spectra were taken after the equilibration of each addition of base using a Varian (Cary 100 BIO) spectrophotometer. The stability constants were refined using the computer program SQUAD.[23]

The IR spectra were obtained using an IR flow cell made of Zn/Se windows and an FTIR Perkin-Elmer 297 spectrophotometer. Spectra corresponding to LyHA (pH 8, $[H_3L^{2+}]_{tot}$ = 0.25 M), mono(L-lysinehydroxamato)tetra(aquo)iron(III) ($[Fe^{3+}]_{tot}$ = 0.50 M, $[H_3L^{2+}]_{tot}$ = 0.25 M, pH 1), and tris(L-lysinehydroxamato)iron(III) ($[Fe^{3+}]_{tot}$ = 0.100 M, $[H_3L^{2+}]_{tot}$ = 0.306 M, pH 6) were all taken in D_2O with anhydrous $FeCl_3$ as the Fe(III) source and the pH adjusted by addition of Na(s).

Rapid ligand dissociation kinetics were measured using an Applied Photophysics stopped-flow instrument (SX.18MV). A pH-jump kinetic method was used, where equal volumes of a solution containing 0.5 mM tris(L-lysinehydroxamato)iron(III) at pH ≈ 6 ($[Fe^{3+}]_{tot}$ = 0.5 mM, $[H_3L^{2+}]_{tot}$ = 5 mM) and one containing an accurately known value of excess perchloric acid solution were mixed and the absorbance decay was recorded at 425 nm for up to 600 s. All kinetic runs were made at T = 25 °C and I = 2.0 M ($NaClO_4/HClO_4$). Kinetic data points represent an average of seven independent kinetic runs. Spartan 5.0[26] software was used to estimate distances within the LyHA molecule to help in kinetic data interpretation.

Cyclic voltammetry measurements were made using a Cypress Systems potentiostat and model CS-1087 computer-controlled electroanalytical system. A ca. 5 mL sample was used in a three-electrode setup, where I = 1.0 M ($NaClO_4$); all solutions were in CH_3CH_2OH/H_2O, 1/1 (v/v), and were purged for 15 min with Ar(g). The auxiliary electrode was a platinum wire polished prior to each experiment. A glassy carbon working electrode was polished sequentially with 5, 1, 0.3, and 0.05 μm alumina and sonicated after each polishing in deionized water to remove the alumina. An aqueous solution of $K_3Fe(CN)_6$ was used to find the area of the working electrode and to calibrate the system ($E_{1/2}$ = 0.458 V vs NHE in 0.5 M KCl).[27] The reference electrode was Ag/AgCl. Redox potentials for tris(L-lysinehydroxamato)iron(III) were obtained at the conditions $[Fe]_{tot}$ = 5 mM, $[LyHA]_{tot}$ = 30 mM, at a scan rate of 20 mV/s with a peak to peak separation of 220 mV and a peak current ratio of 0.8, and $E_{1/2} = (E_c + E_a)/2$. The diffusion coefficient

(15) Rogers, H. J. In *Iron Transport in Microbes, Plants, and Animals*; Winkelmann, G., van der Helm, D., Neilands, J. B., Eds.; VCH: New York, 1987; p 223.
(16) Powers, J. C.; Harper, J. W. In *Proteinase Inhibitors*; Barrett, A. J., Salvesen, G., Eds.; Elsevier: New York, 1986; p 244.
(17) Fishbein, W. N.; Streeter, C. L.; Daly, J. *J. Pharmacol. Exp. Ther.* **1973**, *186*, 173.
(18) Munakata, K.; Kobashi, K.; Takebe, S.; Hase, J. *J. Pharmacobio-Dyn.* **1980**, *3*, 451.
(19) Ramadan, N.; Porath, J. *J. Chromatogr.* **1985**, *321*, 81.
(20) Gran, G. *Acta Chem. Scand.* **1950**, *4*, 559.
(21) Monzyk, B.; Crumbliss, A. L. *J. Am. Chem. Soc.* **1979**, *101*, 6203.
(22) Caudle, M. T.; Crumbliss, A. L. *Inorg. Chem.* **1994**, *33*, 4077.
(23) Gans, P.; Sabatini, A.; Vacca, A. *Inorg. Chim. Acta-Bioinorg. Chem.* **1983**, *79*, 219.
(24) May, P. M.; Williams, D. R.; Linder, P. W.; Torrington, R. G. *Talanta* **1982**, *29*, 249.
(25) Benesi, H. A.; Hildebrand, J. H. *J. Am. Chem. Soc.* **1949**, *71*, 2703.
(26) Wavefunction, Inc., 18401 Von Karman Ave., Suite 370, Irvine, CA 92612.
(27) Kolthoff, I. M.; Tomsicek, W. J. *J. Phys. Chem.* **1935**, *39*, 945.

Table 1. pK_a Values for Various Amino Acids and Aminohydroxamic Acids

compound	α-NH_3	ϵ-NH_3	−C(O)OH	−C(O)NOH	ref
acetic acid	N/A	N/A	4.42	N/A	57
acetohydroxamic acid	N/A	N/A	N/A	9.34	58
glycine	9.76	N/A	2.33	N/A	57
glycinehydroxamic acid	9.19	N/A	N/A	7.43	35
lysine	9.06	10.54	2.19	N/A	59
lysinehydroxamic acid	8.89(1)	10.76(5)	N/A	6.87(1)	*a*

[a] This work, $T = 25$ °C, $I = 0.1$ M ($NaClO_4$).

was calculated from the Randel−Sevcik equation ($i_p = (2.69 \times 10^5)n^{3/2}AD^{1/2}\nu^{1/2}C^o$).

Results

Ligand Proton Dissociation Equilibria. L-Lysinehydroxamic acid (LyHA, H_3L^{2+}) liberates three protons upon titration with NaOH in the pH range of 6.23−11.36. The liberated protons derive from the dissociation of the hydroxamic acid (−NOH), α-NH^{3+}, and ϵ-NH^{3+} moieties. pK_a values at 25 °C and $I = 0.1$ M ($NaClO_4$) are defined in eqs 1−3, where H_3L^{2+} represents the fully protonated LyHA, and are listed in Table 1.

$$H_3L^{2+} \rightleftharpoons H_2L^+ + H^+ \qquad K_{a1} = [H_2L^+][H^+]/[H_3L^{2+}] = 10^{-6.87} \quad (1)$$

$$H_2L^+ \rightleftharpoons HL + H^+ \qquad K_{a2} = [HL][H^+]/[H_2L^+] = 10^{-8.89} \quad (2)$$

$$HL \rightleftharpoons L^- + H^+ \qquad K_{a3} = [L^-][H^+]/[HL] = 10^{-10.76} \quad (3)$$

IR Spectroscopy. The IR spectrum of 0.1 M LyHA in D_2O at pH 8 shows a broad intense ν_{CO} band at 1648 cm^{-1}, in accordance with the carbonyl stretching energies of other hydroxamic acids.[28] A solution of 0.25 M mono(L-lysinehydroxamato)tetra(aquo)iron(III) in D_2O was prepared by the use of excess Fe(III), and the IR spectrum shows the strong ν_{CO} band shifted to lower energy at 1592 cm^{-1}, consistent with the coordination of the carbonyl group to Fe(III). A mixture of bis- and tris(L-lysinehydroxamato)iron(III) complexes was formed at pH 6 with a 1:3 Fe:H_3L^{2+} ratio, and its spectrum contained a ν_{CO} band located between those of the free ligand and the monoligated Fe(III) complex, at 1608 cm^{-1}.

Fe(III) Chelation Equilibria. Elucidation of the LyHA bonding mode requires a determination of the H^+ stoichiometry for mono(L-lysinehydroxamato)tetra(aquo)iron(III) formation. The reaction of LyHA with excess $Fe(H_2O)_6^{3+}$ was monitored spectrophotometrically over the $[H^+]$ range from 0.026 to 0.313 M. The data were analyzed according to a Hill plot of eq 4 based on the equilibrium expression (eq 5), where ϵ is the extinction coefficient of the complex, A is the absorbance, and $Fe(H_{3-n}L)^{(5-n)+}$ is the mono(hydroxamato)tetra(aquo)iron(III) complex of unknown proton stoichiometry. A plot of eq 4 is shown in Figure S-1 of the Supporting Information, where the slope is 1.09, consistent with the displacement of a single proton upon Fe(III) chelation as shown in eq 6 (coordinated waters are omitted for clarity).

Table 2. Stepwise Proton-Dependent (K_n)[a] and Overall Proton-Independent (β_n)[b] Equilibrium Constants for FeL_n Complexes

L	log K_1	log K_2	logK_3	log β_1	log β_2	log β_3	pFe[c]
NMAHA[d]	2.75	0.9	−1.06	11.70	21.50	29.44	16.2
AHA	2.04[e]	0.036[f]	−1.8[f]	11.41[g]	21.01[g]	28.29[g]	12.5
LyHA[h]	−0.0656(8)	−1.3(2)	−3.1(2)	6.80(9)	12.4(2)	16.1(2)	7.1

[a] Defined in eq 16. [b] Defined in eq 12. [c] pH 7.4, $[Fe(III)]_{tot} = 10^{-6}$ M, $[L]_{tot} = 10^{-5}$ M. [d] Reference 22. [e] Reference 21. [f] Reference 60. [g] Reference 61. [h] This work, $T = 25$ °C, $I = 2.0$ M ($NaClO_4$). The numbers in parentheses represent the standard deviation in the last significant figure.

$$\log\{(\epsilon[H_3L^{2+}]_{tot}/A) - 1\} = n \log [H^+] - \log(K_1[Fe^{3+}]) \quad (4)$$

$$K_1 = [Fe(H_{3-n}L)^{(5-n)+}][H^+]^n/[Fe^{3+}][H_3L^{2+}] \quad (5)$$

$$Fe^{3+} + H_3L^{2+} \rightleftharpoons FeH_2L^{4+} + H^+ \qquad K_1 = [Fe(H_2L)^{4+}][H^+]/[Fe^{3+}][H_3L^{2+}] \quad (6)$$

The Benesi−Hildebrand method[25] was used to determine the value of the proton-dependent equilibrium constant described in eq 6. Through rearrangement of eqs 6−10, a linear relationship between $[Fe^{3+}]_{tot}$ and $[Fe^{3+}]_{tot}[H^+]/\{A([H^+] + K_h)\}$ can be established (eq 11 and Figure S-2).

$$[Fe(H_2L)^{4+}] = A/\epsilon \quad (7)$$

$$[Fe^{3+}]_{tot} = [Fe^{3+}] + [Fe(OH)^{2+}] + [Fe(H_2L)^{4+}] \quad (8)$$

$$[H_3L^{2+}]_{tot} = [H_3L^{2+}] + [Fe(H_2L)^{4+}] + [H_2L^+] + [HL] + [L^-] \quad (9)$$

$$Fe^{3+} \rightleftharpoons Fe(OH)^{2+} + H^+ \qquad K_h = [Fe(OH)^{2+}][H^+]/[Fe^{3+}] = 1.51 \times 10^{-3}\ M^{29} \quad (10)$$

$$[Fe]_{tot}[H^+]/\{A([H^+] + K_h)\} = [Fe]_{tot}[H^+]/\{\epsilon[H_3L^{2+}]_{tot}([H^+] + K_h)\} + [H^+]K_1/\epsilon[H_3L^{2+}]_{tot} \quad (11)$$

The slope and intercept of the plot in Figure S-2 of the Supporting Information were used to calculate $\epsilon_{max}(Fe(H_2L)^{4+}) = 814\ M^{-1}\ cm^{-1}$ and K_1(eq 6) = 0.860. From the values of K_1(eq 6) and K_{a1}(eq 1), log $\beta_1 = 6.80(9)$ (eq 12, where $i = 1$; Table 2) may be calculated.

$$\beta_i = [Fe(H_2L)_i^{(3+i)+}]/[Fe^{3+}][H_2L^{2+}]^i \quad (12)$$

The UV−vis spectral characteristics of Fe(III)−hydroxamate complexes are well-known: for one, two, and three hydroxamates in the inner coordination shell, λ_{max} shifts from ∼500 to ∼460 to ∼430 nm and ϵ_{max} increases from ∼1000 to ∼1700−2000 to ∼2500−3000 $cm^{-1}\ M^{-1}$, respectively.[22]

(28) Brown, D. A.; McKeith, D.; Glass, W. K. *Inorg. Chim. Acta* **1979**, *35*, 57.

(29) Milburn, R. M. *J. Am. Chem. Soc.* **1957**, *79*, 537.

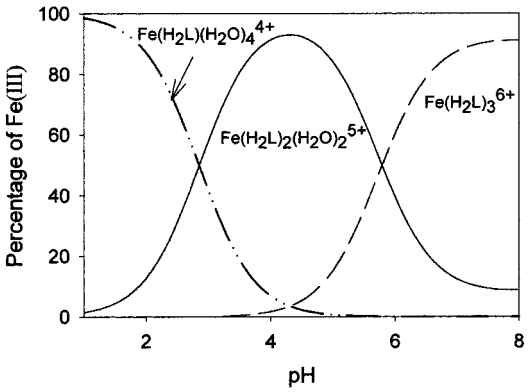

Figure 1. Speciation profile for the LyHA−Fe(III) system at 5 mM LyHA and 0.5 mM Fe(III).

These shifts are easily observable, making UV−vis spectrophotometric titration a viable method for finding the global stability constants for tris(L-lysinehydroxamato)iron(III). Time-dependent UV−vis spectra were collected during the acid-driven dissociation of the tris(LyHA) complex (see below), and the software Pro Kin 1.0 was used to both analyze the collected spectra and calculate individual spectra for the mono-, bis-, and tris(LyHA) complexes (Figure S-3 of the Supporting Information). An isosbestic point was observed at 505 nm in the higher pH region, which was presumably caused by the transition from the tris to bis coordination mode (Figure S-4A of the Supporting Information). This isosbestic point indicates that during the tris to bis transition there are only two species and one mode of coordination present. However, a similar isosbestic point is not observed for the bis to mono conversion (Figure S-4B of the Supporting Information).

A spectrophotometric titration was performed in steady increments from pH 1.19 to pH 8.16. An increase in maximum absorbance and a shift to shorter wavelength is observed as the acid concentration is decreased. Spectra of the solution at pH values above 8.16 begin to show a decrease in maximum absorbance due to the hydrolysis of the complex. SQUAD[23] was used to refine the experimental data according to the reactions described by eqs 13−16,

$$Fe(H_2L)_2^{5+} + H_3L^{2+} \rightleftharpoons Fe(H_2L)_3^{6+} + H^+ \qquad K_3 = k_{-3}/k_3 \tag{13}$$

$$Fe(H_2L)^{4+} + H_3L^{2+} \rightleftharpoons Fe(H_2L)_2^{5+} + H^+ \qquad K_2 = k_{-2}/k_2 \tag{14}$$

$$Fe^{3+} + H_3L^{2+} \rightleftharpoons Fe(H_2L)^{4+} + H^+ \qquad K_1 = k_{-1}/k_1 \tag{15}$$

$$K_i = [H^+][Fe(H_2L)_i^{(3+i)+}]/[Fe(H_2L)_{i-1}^{(3+i)+}][H_3L^{2+}] \tag{16}$$

with K_1 fixed at 0.860 (see above). K_1, K_2, and K_3 values are given in Table 2 along with β_1, β_2, and β_3 values calculated from the corresponding K_n and K_{an} values. The species distribution for Fe(III)/LyHA complexes based on these data is given in Figure 1.

Electrochemistry. Quasi-reversible cyclic voltammograms were obtained for tris(L-lysinehydroxamato)iron(III), where $E_{1/2} = -214$ mV (vs NHE) and the diffusion coefficient is 8.0×10^{-6} cm^2 s^{-1} at 25 °C.

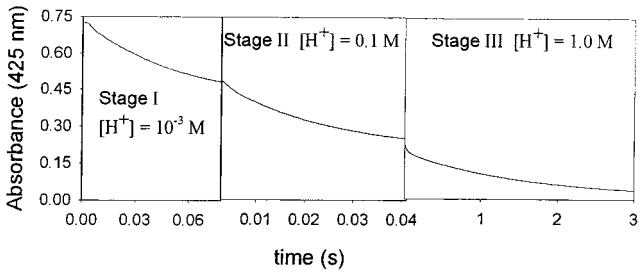

Figure 2. Overall absorbance decay for H^+-initiated ligand dissociation of the tris(L-lysinehydroxamato)iron(III) complex. Conditions: $[Fe^{3+}]_{tot}$ = 0.25 mM; $[LyHA]_{tot}$ = 2.5 mM; I = 2.0 M ($NaClO_4$/$HClO_4$); T = 25 °C; λ = 425 nm; $[H^+] = 1.68 \times 10^{-3}$, 9.6×10^{-2}, and 0.96 M for stages I, II, and III, respectively.

Ligand Dissociation Kinetics. The proton-driven hydrolysis of tris(L-lysinehydroxamato)iron(III) resulted in three distinct steps that were observed at 425 nm under pseudo-first-order conditions of excess $[H^+]$ and ligand (Figure 2). The observed rate constants are presented in Table S-1 of the Supporting Information. The fastest step was on the time scale of 20 ms and was too fast to be observed at high acid concentrations. The second step was best observed in the $[H^+]$ range of 0.0192−0.240 M, and the third step was observed throughout the entire range of acid concentrations. Complete dissociation was not observed when $[H^+] < 1.68 \times 10^{-3}$ M.

The first ligand dissociation step results in a shift in λ_{max} from 425 nm to longer wavelength and lower ϵ_{max}, and corresponds to a tris(L-lysinehydroxamato)iron(III) to bis(L-lysinehydroxamato)di(aquo)iron(III) conversion as illustrated in eq 13. A linear relationship is observed between the apparent dissociation rate constant k_3^{obsd} and $[H^+]$ (Figure S-5 of the Supporting Information). Equations 17 and 18 define a rate law that is consistent with the data in Figure S-5, where the rate constant k_3 listed in Table 3 was obtained from the slope.

$$d[Fe(H_2L)_3^{6+}]/dt = -k_3^{obsd}[Fe(H_2L)_3^{6+}] \tag{17}$$

$$k_3^{obsd} = k_3[H^+] + k_{-3}[H_3L^{2+}] \tag{18}$$

The observed rate constant, k_2^{obsd}, for the second step was also found to vary linearly with $[H^+]$ as shown in Figure S-6 of the Supporting Information. The rate expression in eqs 19 and 20 is consistent with the data in Figure S-6, and the rate constant k_2 corresponding to the ligand dissociation reaction in eq 14 was obtained from the slope (Table 3).

$$d[Fe(H_2L)_2^{5+}]/dt = -k_2^{obsd}[Fe(H_2L)_2^{5+}] \tag{19}$$

$$k_2^{obsd} = k_2[H^+] + k_{-2}[H_3L^{2+}] \tag{20}$$

The third step exhibited a single-exponential absorbance decay associated with reaction 15 and was monitored over a greater range of acid concentrations than the two previously described steps. As seen in the plot of k_1^{obsd} vs $[H^+]$ (Figure 3, inset), at low acid concentrations the apparent rate constant

Table 3. Association (k_{-n}) and Dissociation (k_n) Rate Constants for FeL_n Complexes[a]

L	k_3	k_{-3}[b]	k_2	k_{-2}[b]	k_1	k_{-1}[b]	k_1'	k_{-1}'
NMAHA[c]	8.6×10^3	750	102	810	0.0032	1.8	0.0071	2650
AHA	1.0×10^5 [d]	1700[d]	1400[d]	1600[d]	0.110[d]	12[e]	0.0080[e]	2000[e]
LyHA[f]	$3.0(7) \times 10^4$	24(12)	387(7)	19(9)	0.142(3)	0.122(3)	0.489(2)	$4.5(4) \times 10^2$

[a] All units are M^{-1} s^{-1} except those for k_1', which are s^{-1}; all data collected in solutions containing 2.0 M $NaClO_4/HClO_4$ at 25 °C. [b] Calculated from the equilibrium constant and k_n. [c] Reference 22. [d] Reference 60. [e] Reference 21. [f] This work. The numbers in parentheses represent the standard deviation in the last significant figure.

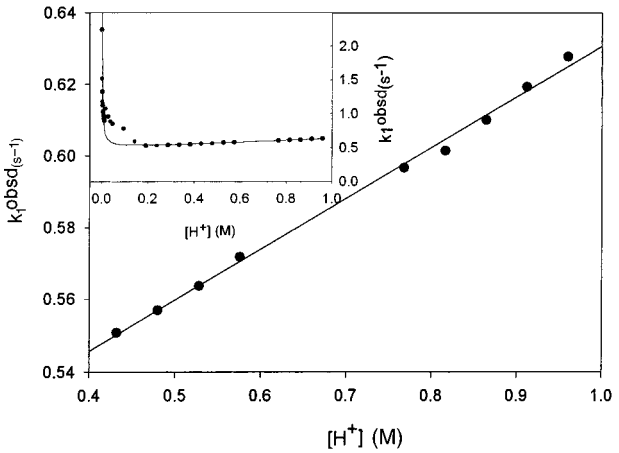

Figure 3. Acid-dependent data for the dissociation of mono(L-lysinehydroxamato)tetra(aquo)iron(III). Conditions: $[Fe^{3+}]_{tot}$ = 0.25 mM; $[LyHA]_{tot}$ = 2.5 mM; I = 2.0 M ($NaClO_4/HClO_4$); T = 25 °C; λ = 425 nm. Data are tabulated in Table S-1. Equation 24 was fit to the data to obtain the parameters a, b, and c, which were plotted as the solid line $k_1^{obsd} = a + b/[H^+] + c[H^+]$, where $a = 0.489(2)$ s^{-1}, $b = 3.4(3) \times 10^{-3}$ M s^{-1}, and $c = 0.142(3)$ M^{-1} s^{-1}.

is inversely proportional to the acid concentration and at higher acid concentrations ($[H^+] > 0.1$ M) the apparent dissociation rate constant varies linearly with $[H^+]$. This behavior is best explained in terms of the parallel paths described by eqs 10, 21−23,

$$FeH_2L^{4+} + H^+ \rightleftharpoons Fe^{3+} + H_3L^{2+} \qquad k_1/k_{-1} \qquad (21)$$

$$FeH_2L^{4+} \rightleftharpoons FeOH^{2+} + H_3L^{2+} \qquad k_1'/k_{-1}' \qquad (22)$$

$$k_1^{obsd} = k_1' + k_1[H^+] + \{2k_{-1}'K_H([Fe^{3+}]_{tot} - [FeH_2L^{4+}])\}/[H^+] \qquad (23)$$

where the relative efficiencies of the paths change from low to high acid concentrations.[22] The solid line in the Figure 3 inset represents a second-order polynomial fit of eq 24, a generic form of eq 23, to the data. At high $[H^+]$, $b/[H^+] \approx$

$$k_1^{obsd} = a + b/[H^+] + c[H^+] \qquad (24)$$

0 and eq 24 simplifies to a linear relationship that is consistent with the data points collected at higher acidity in Figure 3. The results of the linear regression of these data points were used to fix parameters a and c to 0.489 s^{-1} and 0.142 M^{-1} s^{-1}, respectively. The second-order polynomial fit with parameters a and c fixed in this manner produced a value of 3.43×10^{-3} M s^{-1} for parameter b. Parameters a, b, and c, were used to calculate k_1, k_1', and k_{-1}' for reactions 21 and 22 and are listed in Table 3. Also listed in Table 3 is the value for k_{-1}, which was calculated from K_1 and k_1.

Discussion

Ligand Proton Dissociation Equilibria. To assign the pK_a values for LyHA to specific protons, the data were compared to those of L-lysine and other carboxylic and hydroxamic acids listed in Table 1. The pK_a of most hydroxamic acid groups is ca. 9,[30−32] making it possible that any of the pK_a values observed for LyHA could be attributed to the protonation/deprotonation of the hydroxamate group. A comparison of glycine and glycinehydroxamic acid shows a 5.1 log unit increase in pK_a values for the carboxylate to hydroxamate conversion (Table 1). For the same conversion and assuming the same shift on going from L-lysine to LyHA, the new hydroxamate moiety pK_a would be 7.3. A similar carboxylate to hydroxamate comparison is an acetic acid to acetohydroxamic acid conversion that yields a pK_a increase of 4.9 log units. This suggests assigning the pK_a of 6.87 to the hydroxamic acid group of LyHA. The ϵ-amino group should have roughly the same pK_a value for both L-lysine and LyHA; therefore, the pK_a value of 10.76 is assigned to the ϵ-amino group. The last pK_a value of 8.89 is assigned to the α-amino group of LyHA. These LyHA pK_a values were obtained at an ionic strength of 0.1 M $NaClO_4$, and correspond very well to the literature values at ionic strengths of 0.2 M KCl and 0.5 M KCl.[33,34]

Lysinehydroxamic Acid Coordination Mode. Coordination of a carbonyl oxygen atom lone electron pair to a metal center results in a decrease in ν_{CO} due to a decrease in the C═O bond order and an increase in reduced mass. The observed shift in ν_{CO} upon coordination of LyHA to Fe(III) to form mono(L-lysinehydroxamato)tetra(aquo)iron(III) is consistent with carbonyl oxygen atom coordination to Fe(III). A small increase in ν_{CO} (relative to that of the mono complex) for the bis and tris complexes is consistent with a decreased residual positive charge at the Fe center. Evidence of carbonyl oxygen atom coordination, in conjunction with the single H^+ displacement stoichiometry established by the Hill plot (Figure S-1) for reaction 6, is consistent with **IIa** and **IIb** as possible modes of LyHA chelation to Fe(III). The assignment of pK_{a1} to the hydroxamate moiety, comparison of stability constants reported here with other aminohydrox-

(30) Brink, C. P.; Crumbliss, A. L. *J. Org. Chem.* **1982**, *47*, 1171.
(31) Brink, C. P.; Fish, L. L.; Crumbliss, A. L. *J. Org. Chem.* **1985**, *50*, 2277.
(32) Monzyk, B.; Crumbliss, A. L. *J. Org. Chem.* **1980**, *45*, 4670.
(33) O'Sullivan, P.; Glennon, J. D.; Farkas, E.; Kiss, T. *J. Coord. Chem.* **1996**, *38*, 271.
(34) Leporati, E. *J. Coord. Chem.* **1993**, *28*, 173.

amic acids,[35] and pH-dependent shifts in λ_{max} values for solutions containing Fe^{3+}(aq) and LyHA strongly support **IIa** as the probable mode of LyHA chelation to Fe(III).

Fe(III) Chelation Equilibria. The equilibrium constants for the stepwise chelation of Fe(III) by LyHA are compared with the two prototypical monohydroxamic acids acetohydroxamic acid (AHA) and *N*-methylacetohydroxamic acid (NMAHA) in Table 2. Both stepwise proton-dependent (K_i, eq 16) and overall proton-independent (β_I, eq 12) constants for the formation of $Fe(H_2L)(H_2O)_4^{4+}$, $Fe(H_2L)_2(H_2O)_2^{5+}$, and $Fe(H_2L)_3^{6+}$ are lower than corresponding values for the NMAHA and AHA complexes. This is due to one or more of the four major differences among NMAHA, AHA, and LyHA: (i) the lower pK_a value for the chelating hydroxamate group in LyHA, (ii) the higher overall positive charge on the Fe−LyHA complex, (iii) the presence of an α-amine moiety in the Fe−LyHA complex, and (iv) the *N*-substituent (H in LyHA and AHA, and CH_3 in NMAHA). The tris complex for NMAHA and AHA has a neutral charge, whereas the tris complex for LyHA has a large positive charge (+6). This net positive charge leads to a significant charge−charge repulsion and an overall decrease in the stability of the tris(LyHA)−Fe(III) complex. There are analogous charge differences for comparison of the mono and bis complexes, although the magnitude of the charge differential is less for the bis and mono complexes: +1 vs +5 and +2 vs +4 for the bis and mono complexes for NMAHA or AHA, and LyHA, respectively.

The lower pK_a value for the hydroxamate group of LyHA relative to AHA and NMAHA is consistent with LyHA being a weaker O donor due to the electronic effect of the α-ammonium moiety. Consequently, LyHA forms a less stable Fe(III) complex as illustrated by the fact that there is a linear relationship between pK_a and log β_1 (slope 0.5, data not shown) for the N−H hydroxamate ligands L-lysinehydroxamic acid, acetohydroxamic acid, benzohydroxamic acid, and *p*-methoxybenzohydroxamic acid.

LyHA, AHA, and NMAHA exhibit the two resonance forms shown in eq 25.[22,36] In resonance form **IIIb**, the nitrogen atom has a positive charge that can be stabilized by the presence of an electron-donating group at the R_N position. Stabilization of the **IIIb** form will increase the donor

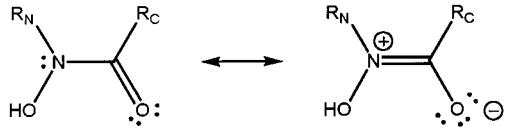

(25)

IIIa **IIIb**

character of the carbonyl group and result in a more stable Fe(III) complex and a slower ligand dissociation rate for the Fe(III) complex. The electron-donating methyl group on the N atom will stabilize the **IIIb** resonance structure of NMAHA and therefore lend additional stability to the NMAHA−Fe(III) complexes. AHA and NMAHA only differ with respect to the *N*-substituent, and it is observed that the NMAHA stability constants and pFe values are about 1 and 4 orders of magnitude higher, respectively. The last column in Table 2 represents the pFe values for AHA, NMAHA, and LyHA (−(log [Fe^{3+}]) at 1 μM Fe^{3+} and 10 μM ligand at pH 7.4).[2] pFe values are a more direct comparison of ligand binding strength in solution, since pK_a, stoichiometry, and denticity effects are taken into account in the calculation. Comparing the pFe values of LyHA and AHA, there is over a 5 order of magnitude difference that is attributed to the overall charge difference, pK_a difference, and presence of the α-amine group on LyHA.

Table 4. Overall Equilibrium Constants for Fe(III)−Aminohydroxamate Complexes

log β_{FeHL}	LyHA[a]	Hisha[b]	Argha[c]	α-Alaha[d]	Glyha[e]	Metha[f]	Glu-δ-ha[g]
log β_{111}[h]	15.69(9)	18.07	16.06	17.15	17.36	16.26	18.92
log β_{122}[i]	30.2(2)	31.37	31.04			30.94	36.65
log β_{133}[j]	42.8(2)				48.28		

[a] L-lysine hydroxamic acid, this work. [b] Histidinehydroxamic acid, ref 62. [c] Argininehydroxamic acid, ref 63. [d] α-Alaninehydroxamic acid, ref 64. [e] Glycinehydroxamic acid, ref 65. [f] Methioninehydroxamic acid, ref 66. [g] Glutamic acid-δ-hydroxamic acid, ref 37. [h] β_{111} = [Fe(HL)]/[Fe][L][H] or [$Fe(H_2L)$]/[Fe][HL][H]. [i] β_{122} = [$Fe(HL)_2$]/[Fe][L]^2[H]^2 or [$Fe(H_2L)_2$]/[Fe][HL]^2[H]^2. [j] β_{133} = [$Fe(HL)_3$]/[Fe][L]^3[H]^3 or [$Fe(H_2L)_3$]/[Fe][HL]^3[H]^3.

To compare LyHA−Fe(III) formation constants with literature data for Fe(III) complexes of other α-amino hydroxamic acids, β_{FeHL} values corresponding to eqs 26−28 were computed for L-lysinehydroxamic acid. These data

$$Fe^{3+}(aq) + H^+ + HL \rightleftharpoons Fe(H_2L)^{4+}$$
$$\beta_{111} = [Fe(H_2L)^{4+}]/[HL][Fe^{3+}(aq)][H^+] \quad (26)$$

$$Fe^{3+}(aq) + 2H^+ + 2HL \rightleftharpoons Fe(H_2L)_2^{5+}$$
$$\beta_{122} = [Fe(H_2L)_2^{5+}]/[HL]^2[Fe^{3+}(aq)][H^+]^2 \quad (27)$$

$$Fe^{3+}(aq) + 3H^+ + 3HL \rightleftharpoons Fe(H_2L)_3^{6+}$$
$$\beta_{133} = [Fe(H_2L)_3^{6+}]/[HL]^3[Fe^{3+}(aq)][H^+]^3 \quad (28)$$

are presented in Table 4 along with the corresponding literature data. LyHA, Hisha, and Argha are positively charged as ligands, whereas α-Alaha, Glyha, and Metha are all neutral Fe(III) binding ligands. Within the group of amine hydroxamates (LyHA, Hisha, Argha, Alaha, Glyha) there is no discernible effect of charge on complex stability, with the possible exception of $Fe(glyha)_3^{3+}$. The larger stability constants for Glu-δ-ha−Fe(III) complexes compared to the other aminohydroxamic acids is attributed to higher Fe(III) chelating denticity.[37] The fact that the stability constants for the Fe(III) complexes of LyHA are consistent with those of the other aminohydroxamic acids adds further support that LyHA binds Fe(III) through the hydroxamate group (O,O) as shown in **IIa**. Hydroxamate binding for LyHA was also

(35) Kurzak, B.; Kozlowski, H.; Farkas, E. *Coord. Chem. Rev.* **1992**, *114*, 169.
(36) Brown, D. A.; Glass, W. K.; Mageswaran, R.; Girmay, B. *Magn. Reson. Chem.* **1988**, *26*, 970.
(37) Farkas, E.; Buglyo, P. *GERA, Proc. 28th Int. Conf. Coord. Chem.* **1990**, *1*, 30.

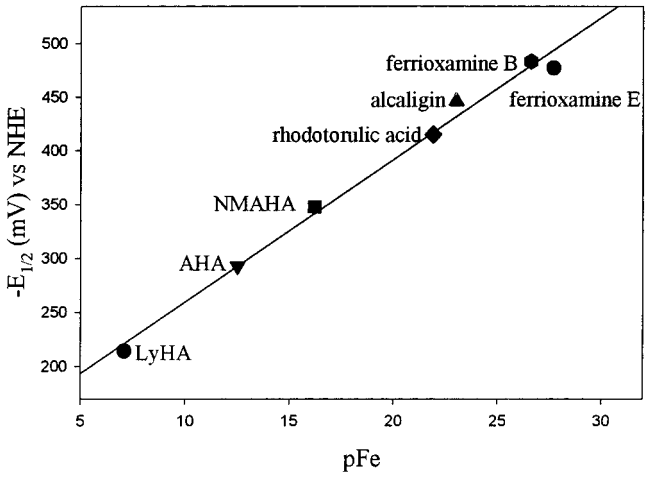

Figure 4. $-E_{1/2}$ vs pFe for various hydroxamic acid complexes of Fe(III). Data for ferrioxamine B, ferrioxamine E, alcalign, rhodotorulic acid, and NMAHA are from ref 39.

concluded previously from equilibrium constants reported by Kujundžić and Inic.[38]

We have previously shown that there is a linear relationship between reduction potential ($E_{1/2}$) and pFe values for Fe(III) complexes of hydroxamic acids.[39] This report extends that relationship by almost 10 orders of magnitude and indicates that the large positive shift in $E_{1/2}$ for tris(L-lysinehydroxamato)iron(III) relative to the other trishydroxamate complexes is due to the lower stability of this complex (Figure 4).

Ligand Exchange Kinetics. Rate constant data for the proton-driven stepwise dissociation of $Fe(LyHA)_3^{6+}$, along with $Fe(AHA)_3$ and $Fe(NMAHA)_3$, are summarized in Table 3. As has been observed for other trischelate complexes of Fe(III),[1,40] proton-driven stepwise dissociation of each ligand proceeds with decreasing second-order rate constants. Proton attack on the hydroxamate is the driving force for Fe(III) release in the proposed mechanism. Rate constants for the dissociation of the NMAHA ligand are smaller, due to the additional kinetic stability observed for hydroxamic acid complexes with electron-releasing *N*-alkyl substituents.[22] The tris(L-lysinehydroxamato)iron(III) complex has a +6 charge, whereas the analogous AHA and NMAHA complexes have a neutral charge. For a positively charged proton to attack the tris(L-lysinehydroxamato)iron(III) complex, it must overcome the charge−charge repulsion generated from the large positive charge on the complex. This barrier is nonexistent for the tris(AHA)− and tris(NMAHA)−Fe(III) complexes. With the loss of each ligand, the charge difference between the LyHA and AHA or NMAHA complexes becomes smaller, (+6 vs 0 for the trishydroxamate, +5 vs +1 for the bishydroxamate, and +4 vs +2 for the monohydroxamate complexes) and the difference in proton repulsion also becomes smaller. This effect can be observed in the complex dissociation rate constants. The ratios of k_n(AHA)/k_n(LyHA) are 3.4, 3.6, and 0.77 for $n = 3$, 2, and 1, respectively. The reason for the low ratio for k_1 may be due to the enhanced ease of dissociating a +2-charged ligand (LyHA) from a +3-charged complex ($Fe(H_2O)_6^{3+}$), relative to an uncharged ligand (AHA) from a +3-charged complex. The end result of this charge differential is that the rate of dissociation for the mono(LyHA) complex ($Fe(H_2L)(H_2O)_4^{4+}$) is actually slightly faster than that of the corresponding AHA complex.

The trends in complex formation rate constants shown in Table 3 are similar for LyHA, AHA, and NMAHA. Reactivity at $Fe(H_2O)_5OH^{2+}$ is higher than at $Fe(H_2O)_6^{3+}$ (k_{-1}' vs k_{-1}) due to the higher rate of water exchange at $Fe(H_2O)_5OH^{2+}$.[41−43] Ligand substitution rates generally increase on formation of the mono, bis, and tris complexes, presumably due to the labilizing effect of the hydroxamate ligand on the remaining coordinated waters. A striking feature of the complex formation rate constant data in Table 3 is the significantly smaller rate constants (k_{-1}, k_{-1}', k_{-2}, k_{-3}) for LyHA relative to AHA and NMAHA, despite the fact that these reactions should be dissociatively activated (i.e., largely dependent on the dynamics of the leaving water ligand). Although the entering chelating moiety is the same in each case, LyHA differs from AHA and NMAHA in that it carries a +2 charge. As demonstrated below, it is this difference in electrostatics that is controlling the relative rates of complex formation for these three hydroxamic acids.

The Eigen−Wilkins[44−46] model for complex formation is a two-step process whereby a rapid preequilibrium is reached to form an outer-sphere association complex, followed by the rate-determining ligand exchange step (eqs 29 and 30).

$$Fe(H_2O)_6^{3+} + L \overset{K_{OS}}{\rightleftharpoons} Fe(H_2O)_6^{3+} + L \xrightarrow{k_{-n}} Fe(H_2O)_4L^{n+} + 2H_2O \quad (29)$$

$$k_{-n} = Sk_wK_{OS} \quad \text{where}$$

$$K_{OS} = [Fe(H_2O)_6^{3+}, L]/[L][Fe(H_2O)_6^{3+}] \quad (30)$$

In eq 30 k_w is the rate of water exchange and L is a bidentate ligand where initial bond formation is rate determining and chelate ring closure is rapid. The rate constant for a dissociative interchange activated ligand exchange can be approximated by the rate constant for water exchange (k_w) at $Fe(H_2O)_6^{3+}$, modified by an outer-sphere association constant (K_{OS}) and a statistical correction (S) that accounts for the fraction of water dissociations that actually lead to ligand (L) substitution. The Eigen−Wilkins model is reasonable for this case since ligand exchange at aquated Fe^{3+} is an interchange process (I) with some evidence for mild associative activation (I_a) at $Fe(H_2O)_6^{3+}$ and dissociative activation (I_d) at $Fe(H_2O)_5OH^{2+}$.[40,47]

(38) Kujundžić, N.; Inic, S.; Todoric-Kovacević, V. *Acta Pharm. (Zagreb)* **1994**, *44*, 61.
(39) Spasojević, I.; Armstrong, S. K.; Brickman, T. J.; Crumbliss, A. L. *Inorg. Chem.* **1999**, *38*, 449.
(40) Biruš, M.; Kujundžić, N.; Pribanić, M. *Prog. React. Kinet.* **1993**, *18*, 171.
(41) Dodgen, H. W.; Liu, G.; Hunt, J. P. *Inorg. Chem.* **1981**, *20*, 1002.
(42) Grant, M.; Jordan, R. B. *Inorg. Chem.* **1981**, *20*, 55.
(43) Swaddle, T. W.; Merbach, A. E. *Inorg. Chem.* **1981**, *20*, 4212.
(44) Eigen, M.; Tamm, K. *Z. Elektrochem.* **1962**, *66*, 93.
(45) Eigen, M.; Wilkins, R. G. *Adv. Chem. Ser.* **1965**, *49*, 55.
(46) Eigen, M. *Ber. Bunsen-Ges. Phys. Chem.* **1963**, *67*, 753.

The validity of eq 30 and the application of the Eigen−Wilkins mechanism to the Fe(III)−LyHA system can be evaluated by using experimental k_w values for $Fe(H_2O)_6^{3+}$ and $Fe(H_2O)_5OH^{2+}$ [41−43] and estimated values for K_{OS}[48] to calculate values for k_{-1} and k_{-1}', which may then be compared with the experimental k_{-1} and k_{-1}' values. K_{OS} can be estimated using the Fuoss equation (eq 31) and the Debye−Hückel interionic potential (eqs 32 and 33),

$$K_{OS} = (4\pi Na^3/3000)\exp(-U(a')/kT) \quad (31)$$

$$U(a') = z_1z_2e^2/a'D - z_1z_2e^2\kappa/(D(1+\kappa a')) \quad (32)$$

$$\kappa^2 = 8\pi Ne^2\mu/(1000DkT) \quad (33)$$

where N is Avogradro's number, a is the center-to-center distance of closest approach of the two ions (cm), a' is the distance between the center of positive charge on the metal and the center of positive or negative charge on the incoming ligand (cm), k is Boltzmann's constant (ergs), e is the charge on an electron (esu), D is the dielectric constant, μ is the ionic strength, and z_1 and z_2 are the charges of the metal complex and entering ligand.[48−50] To solve eq 31 for K_{OS}, the dielectric constant for 2.0 M $NaClO_4$ was assumed to be 53.44,[51] and the closest distance between the two ion centers (a) was estimated to be 4 Å. The value of 4 Å has been calculated previously from X-ray diffraction studies of $Fe(OH_2)_6^{3+}$.[47,52,53] There are two differences in the calculations for LyHA, and AHA or NMAHA: the charges on the ligands and the distance used for a'. For AHA and NMAHA $a = a'$, but for LyHA $a \neq a'$. A series of calculations using the Spartan 5.0 software and different models produced a range of a' values for LyHA from 7.0 to 8.4 Å. An average value of 7.7 Å was taken to calculate K_{OS}. For the formation of the mono(L-lysinehydroxamato)tetra(aquo)iron(III) complex, the important pairs of charges are +3, +2 (for reaction with $Fe(H_2O)_6^{3+}$) and +2, +2 (for reaction with $Fe(H_2O)_5OH^{2+}$), whereas the charges for the mono(AHA)− and mono(NMAHA)−Fe(III) complexes are +3, 0 and +2, 0, respectively. Values were calculated for k_{-1} and k_{-1}' using eq 30 and the K_{OS} values from eq 31;[54] $k_w = 160\ s^{-1}$ for $Fe(H_2O)_6^{3+}$ and $1.2 \times 10^5\ s^{-1}$ for $Fe(H_2O)_5OH^{2+}$.[41−43] To obtain good agreement between the calculated and experimental values of k_{-1} and k_{-1}' for AHA and NMAHA, S was assumed to be 1/8 (calculated values: k_{-1}(AHA or NMAHA) = 3.2 $M^{-1}\ s^{-1}$ and k_{-1}'(AHA or NMAHA) = 2400 s^{-1}; cf. experimental values in Table 3). The ability of a ligand to chelate a metal is dependent on its position in the second coordination sphere and the orientation of its chelating moiety. For the former an S value of 1/3 is consistent with each edge of the octahedron serving as a site for the incoming ligand in the second coordination sphere and each dissociating water being adjacent to four edges.[50] An additional decrease in the rate constant can be attributed to steric hindrance or the possibility that the chelating moiety is in the improper orientation. Hence, $S = 1/8$ is a reasonable statistical correction for substitution reactions of AHA and NMAHA. A similar analysis for LyHA reveals an S value of ca. 1/20 (calculated values: k_{-1}(LyHA) = 0.28 $M^{-1}\ s^{-1}$ and k_{-1}'(LyHA) = 350 s^{-1}; cf. experimental values in Table 3). The statistical factor (S) for LyHA is composed of the same components as that for NMAHA and AHA. As expected, the steric demands for entry of the larger dication LyHA are more critical than those for NMAHA or AHA; consequently, S is smaller. Overall, there is excellent agreement between calculated and experimental values (Table 3), which lends credibility to the mechanism described by eqs 29 and 30. That is, monohydroxamate Fe(III) complex formation follows the Eigen−Wilkins model whereby the rate constant for complex formation is controlled by the water exchange rate constant k_w at $Fe(H_2O)_6^{3+}$ and $Fe(H_2O)_5OH^{2+}$, after corrections for solvent shell composition (S) and for entering ligand charge (K_{OS}).

The ratios of experimental rate constants k_{-n}(LyHA)/k_{-n}(AHA) and k_{-n}(LyHA)/k_{-n}(NMAHA) for formation of the mono ($FeL(H_2O)_4^{z+}$), bis ($FeL_2(H_2O)_2^{z+}$), and tris (FeL_3^{z+}) complexes are all consistent (within a factor of <3, Table 3) with the values of the ratios being controlled by the ratios of the K_{OS} values. That is, the relative rates of the formation reaction steps are largely controlled by electrostatic factors, consistent with an interchange process. Distinction between dissociative and associative activation (I_d and I_a) is not possible since in all cases the attacking moiety is a hydroxamic acid.

The kinetics and thermodynamics for the stepwise dissociation of L-lysinehydroxamic acid from $Fe(LyHA)_3^{6+}$ may be summarized and compared with the corresponding reactions of $Fe(AHA)_3$ and $Fe(NMAHA)_3$ through a plot of ln k_{diss} vs ln K_{diss}, where k_{diss} and K_{diss} are the rate and equilibrium constants for the stepwise dissociation of Fe(hydroxamate)$_3$ to give $Fe(H_2O)_6^{3+}$. Such a plot is shown in Figure 5. Rather than a quantitative analysis of this linear free energy relationship (LFER), we are interested in pattern recognition and what can be concluded concerning (1) the mechanistic similarities among the dissociations of the first, second, and third hydroxamate ligands from $Fe(L)_3$ and (2) the mechanistic similarities among ligand dissociations from Fe(III) complexes of lysinehydroxamic acid, *N*-methylacetohydroxamic acid, and acetohydroxamic acid. Figure 5 should be considered as illustrative of the trends in the data. Rather than consideration as a single quantitative relationship, Figure 5 may be viewed as a cluster of three related plots, one for the ligand dissociation data for $Fe(L)_3^{z+}$ (cluster I, data points 1−3), another for the ligand dissociation data for $Fe(L)_2(H_2O)_2^{z+}$ (cluster II, data points 4−6), and another

(47) Crumbliss, A. L.; Garrison, J. M. *Comments Inorg. Chem.* **1988**, *8*, 1.
(48) Fuoss, R. M. *J. Am. Chem. Soc.* **1958**, *80*, 5059.
(49) Eigen, M. *Z. Phys. Chem. (Frankfurt)* **1954**, *1*, 176.
(50) Lin, C.-T.; Rorabacher, D. B. *Inorg. Chem.* **1973**, *12*, 2402.
(51) Barthel, J.; Buchner, R.; Munsterer. *Electrolyte Data Collection; Part 2: Dielectric Properties of Water and Aqueous Electrolyte Solutions*; Chemistry Data Series; DECHEMA: Frankfurt, Germany, 1995; Vol XII, Part 2, p 206.
(52) Caminiti, R.; Magini, M. *Chem. Phys. Lett.* **1979**, *61*, 40.
(53) Hair, N. J.; Beattie, J. K. *Inorg. Chem.* **1976**, *16*, 245.
(54) K_{OS} values for (z_1, z_2) ion pairs calculated from eq 31 where $a = 4$ Å, $a' = 7.7$ Å, $D = 53.44$, and $I = 2.0$ M are (+2, +2) 0.0582 M^{-1} and (+2, +3) 0.0349 M^{-1}, and K_{OS} values for (z_1, z_2) ion pairs calculated from eq 31 where $a = a' = 4$ Å, $D = 53.44$, and $I = 2.0$ M are (0,+2) 0.161 M^{-1} and (0,+3) 0.161 M^{-1}.

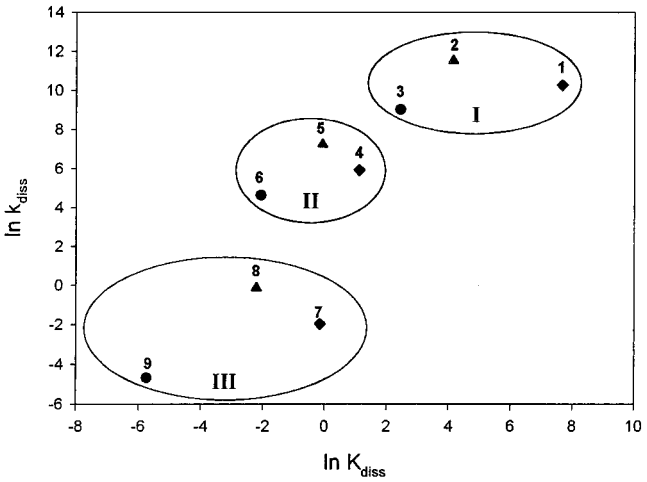

Figure 5. ln k_{diss} vs ln K_{diss} (eq 35) for Fe(III) dissociation reactions with hydroxamic acid ligands LyHA, NMAHA, and AHA. All data were measured in aqueous 2.0 M $NaClO_4/HClO_4$ at 25 °C. Data are from Tables 2 and 3. Key: (◆) LyHA, (●) NMAHA, (▲) AHA, (1) $Fe(LyHA)_3^{6+}$, (2) $Fe(AHA)_3$, (3) $Fe(NMAHA)_3$, (4) $Fe(LyHA)_2(H_2O)_2^{5+}$, (5) $Fe(AHA)_2(H_2O)_2^{+}$, (6) $Fe(NMAHA)_2(H_2O)_2^{+}$, (7) $Fe(LyHA)(H_2O)_4^{4+}$, (8) $Fe(AHA)(H_2O)_4^{2+}$, and (9) $Fe(NMAHA)(H_2O)_4^{2+}$.

for the ligand dissociation data for $Fe(L)(H_2O)_4^{z+}$ (cluster III, data points 7−9). The mechanistic conclusions that may be made through an analysis of the LFER shown in Figure 5 are discussed below in a qualitative sense.

An LFER that correlates rate and equilibrium constants implies a mathematical relationship such as shown in eq 34.

$$k = \alpha K^{\beta} \tag{34}$$

For a dissociative process where the departing/entering hydroxamic acid ligand does not influence the free energy of the transition state, one may expect a linear relationship between ln k_{diss} and ln K_{diss} with a unit slope according to eq 35. This is in the form of Figure 5 and represents an expansion of eq 34.

$$\ln k_{diss} = \ln k_{form} + \ln K_{diss} \tag{35}$$

A number of observations concerning Figure 5 are evident. First, the ligand (L) dissociation rate constants, k_{diss}, for all FeL_x increase on going from $FeL(H_2O)_4^{z+}$ to $Fe(L)_2(H_2O)_2^{z+}$ to $Fe(L)_3^{z+}$, but not linearly (cf. data points (9, 6, 3), (8, 5, 2), and (7, 4, 1)). This suggests that while the water exchange rates increase as expected on going from $Fe(H_2O)_6^{3+}$ to $Fe(L)(H_2O)_4^{z+}$ to $Fe(L)_2(H_2O)_2^{z+}$ for a given ligand, they do not do so linearly and tend to saturate in the bis complex. This trend is also observed in tris(tiron)− and tris(hydroxyquinoline)−Fe(III) complexes.[55,56] Second, according to the Eigen−Wilkins mechanism, k_{form} in eq 35 may be described as shown in eq 30, where S is a statistical factor, K_{OS} is the diffusion-controlled outer-sphere association constant, and k_w is the water exchange constant for $Fe(H_2O)_6^{3+}$, $Fe(L)(H_2O)_4^{z+}$, and $Fe(L)_2(H_2O)_2^{z+}$. Within the context of eqs 30 and 35, a number of features of Figure 5 are now evident. First, the intercept should be different for each cluster (cluster I, data points 1−3; cluster II, data points 4−6; cluster III, data points 7−9) because k_w will be different for $Fe(H_2O)_6^{3+}$, $Fe(L)(H_2O)_4^{z+}$, and $Fe(L)_2(H_2O)_2^{z+}$. Second, the intercept for the data clusters associated with the ligand dissociation from $Fe(L)(H_2O)_4^{z+}$, $Fe(L)_2(H_2O)_2^{z+}$, and $Fe(L)_3^{z+}$ should increase because of k_w increasing for $Fe(H_2O)_6^{3+}$, $Fe(L)(H_2O)_4^{z+}$, and $Fe(L)_2(H_2O)_2^{z+}$, but not necessarily linearly. Third, the intercept should be approximately the same for L = AHA and NMAHA, but different for L = LyHA (due to electrostatic factors discussed above and amplified further below).

Since in eq 30 k_w should be roughly the same for the AHA, NMAHA, and LyHA complexes, the intercept according to eq 35 should vary with SK_{OS}. Consequently, we expect the LyHA ligand dissociation data to fall below a line of unit slope defined by the AHA and NMAHA complexes. This pattern is observed in Figure 5. The magnitude of this deviation in each case can be estimated from $\ln((S)(K_{OS}^{L})/(S)(K_{OS}^{LyHA}))$ (L = AHA, NMAHA). From the calculated K_{OS} values[54] it is estimated that the LyHA complex data point should fall 3.5, 3.0, and 2.4 ln units below the line defined by the AHA and NMAHA complex systems for ligand dissociation from $Fe(L)_3^{z+}$, $Fe(L)_2(H_2O)_2^{z+}$, and $Fe(L)(H_2O)_4^{z+}$, respectively. Although not strictly obeyed in Figure 5, the predicted trend is certainly present.

Conclusions

LyHA was found to bind Fe(III) exclusively through the hydroxamate moiety, thereby leaving the two amine groups free to potentially act as recognition agents. The pK_a of the hydroxamate moiety is lowered due to the electron-withdrawing α-amine moiety. Consequently, this α-amine is responsible for the lower stability of the LyHA−Fe(III) complexes relative to AHA and NMAHA complexes of Fe(III) and contributes to the observed charge effects. The influence of ligand charge on ligand exchange kinetics and thermodynamics was investigated by comparing results obtained for the dication $LyHA^{2+}$ with the corresponding processes involving AHA and NMAHA. Ligand charge was found to shift the redox potential for $Fe(LyHA)_3^{6+}$ positive relative to those of other Fe(III)−hydroxamate complexes. As the charge on the complex is increased, a corresponding decrease in the rate of ligand dissociation is observed when

(55) Zhang, Z.; Jordan, R. B. *Inorg. Chem.* **1996**, *35*, 1571.
(56) Boukhalfa, H.; Thomas, F.; Serratrice, G.; Beguin, C. G. *Inorg. React. Mech.*, in press.
(57) Perrin, D. D. *Stability Constants of Metal-Ion Complexes: Part B Organic Ligands*; Pergamon Press: New York, 1979.
(58) Martell, A. E.; Smith, R. M. *Critical Stability Constants*; Plenum Press: New York, 1974; Vol. 3.
(59) Sillen, L. G.; Martell, A. E. *Stability Constants of Metal-Ion Complexes: Part 1. Inorganic Ligands*; Burlington House: London, 1971; Vol. 25.
(60) Biruš, M.; Bradić, Z.; Kujundžić, N.; Pribanić, M.; Wilkins, P. C.; Wilkins, R. G. *Inorg. Chem.* **1985**, *24*, 3980.
(61) Schwarzenbach, G.; Schwarzenbach, K. *Helv. Chim. Acta* **1963**, *46*, 1390.
(62) Brown, D. A.; Sekhon, B. S. *Inorg. Chim. Acta* **1984**, *91*, 103.
(63) Leporati, E.; Nardi, G. *Gazz. Chim. Ital.* **1991**, *121*, 147.
(64) Farkas, E.; Szoke, J.; Kiss, T.; Kozlowski, H.; Bal, W. *J. Chem. Soc., Dalton Trans.* **1989**, 2247.
(65) El-Ezaby, M. S.; Hassan, M. M. *Polyhedron* **1985**, *4*, 429.
(66) El-Ezaby, M. S.; Marafie, H. M.; Abu-Soud, H. M. *Polyhedron* **1986**, *5*, 973.

the LyHA system is compared to the corresponding complexes of AHA and is attributed to charge−charge repulsion between the complex and the incoming H^+. This electrostatic repulsion also affects the rate of formation, whereby the formation of $Fe(LyHA)_x(H_2O)_{6-2x}^{(3+x)+}$ is consistent with the Eigen−Wilkins model for ligand exchange mediated by charge effects.

Acknowledgment. Financial support from the NSF and the American Chemical Society Petroleum Research Fund is gratefully acknowledged.

Supporting Information Available: A table of observed rate constants for ligand dissociation from tris(L-lysinehydroxamato)-iron(III) and six figures showing the Hill plot for eq 4, Benesi−Hildebrand method plot for eq 11, absorbance spectra for mono-, bis-, and tris(L-lysinehydroxamato)iron(III), UV−vis spectra of tris(L-lysinehyroxamato)iron(III) ligand dissociation, and kinetic data for dissociation of tris(L-lysinehydroxamato)iron(III) and bis(L-lysinehyroxamato)di(aquo)iron(III). This material is available free of charge via the Internet at http://pubs.acs.org.

IC0109795